Scattering Vector Dependence of Mutual Diffusion Coefficients for Rodlike Micelles in Aqueous Sodium Halide Solutions

Toyoko Imae

Department of Chemistry, Faculty of Science, Nagoya University, Chikusa, Nagoya 464, Japan
(Received: September 27, 1988; In Final Form: March 8, 1989)

The dynamic light scattering for aqueous sodium halide solutions of heptaoxyethylene alkyl ethers (C_nE_7, n = 10, 12, 14, 16) and tetradecyldimethylammonium chloride and bromide (C_{14}DAC, C_{14}DAB) has been measured at various scattering angles. The scattering vector dependence of mutual diffusion coefficients can be classified into several types, relating with regimes of micelle concentration, that is, dilute, semidilute, and concentrated regimes. The curves with positive initial slopes are contributed to by the rotational diffusion besides the translational diffusion. On the other hand, curves with negative initial slopes are mainly originated by the translational diffusion and its anisotropy.

Introduction

Recently, many workers have been investigating the dynamic light scattering of aqueous micellar solutions. Nevertheless, there are very few reports associating with the scattering vector dependence of mutual diffusion coefficients for aqueous micellar solutions.

Flamberg and Pecora[1] have measured the dynamic light scattering for 4 M NaCl solutions of dodecyldimethylammonium chloride. The measurements were carried out at four scattering angles, and results were analyzed on the basis of the scattering theory for very large molecules.

Wilcoxon and Kaler[2] have reported the dynamic light scattering measurement for aqueous solution of hexaoxyethylene dodecyl ether with the surfactant concentration of 1.3×10^{-2} g cm^{-3} at several temperatures. They revealed that mutual diffusion coefficients increased with an upward convex curvature, as the square of the magnitude of scattering vector, $\mu^2 = [(2\pi\tilde{n}_0/\lambda) \sin(\theta/2)]^2$, increased, where $\tilde{n}_0$ is the refractive index of solvent, λ is the wavelength of incident light, and θ is the scattering angle.

The dynamic light scattering for large molecules was theoretically formulated by a few workers. Pecora and co-workers[3-6] derived equations of the field correlation function for flexibly coiled, rigid rod, and wormlike polymer chains in dilute solutions and rigid rod polymer molecules in semidilute solutions. Fujime and Maeda[7-9] described theoretically the field correlation function from dilute, semidilute, and concentrated solutions of very long semiflexible filaments. Theories were applied to solutions of poly(γ-benzyl L-glutamate)s[5,10] and suspensions of fd virus.[9]

In the present paper, the dynamic light scattering is measured at various scattering angles for aqueous sodium halide solutions of nonionic and cationic surfactants in dilute, semidilute, and concentrated regimes. The dependence on scattering vector of mutual diffusion coefficients is classified into different types and is related with micelle concentration.

It has been confirmed that rodlike micelles are formed in aqueous sodium halide solutions of C_nE_7, C_{14}DAC, and C_{14}DAB examined here.[11-14] Long rodlike micelles exhibited a semiflexible character in dilute solutions and were overlapped and entangled one another in semidilute solutions. Micelles in the concentrated regime behaved differently from those in the semidilute regime. Therefore, the scattering vector dependent dynamic light scattering for aqueous solutions of rodlike micelles in this work is discussed on the basis of the theory for semiflexible polymer chains in dilute, semidilute, and concentrated regimes.

Experimental Section

C_nE_7, C_{14}DAC, and C_{14}DAB were the same samples as previously used.[11-16] NaCl and NaBr were heated for 1 h. Water was redistilled from alkaline potassium permanganate.

The dynamic light scattering was measured at a 488-nm wavelength on an Otsuka Denshi dynamic light scattering spectrophotometer DLS-700.[11,16] The scattering angle was changed from 20 to 150°. The temperature of the cell housing was varied between 20 and 45 °C. Solutions were filtered five times through a Millipore membrane filter.

The second-order field correlation function was measured in the homodyne mode. The first-order normalized autocorrelation function was analyzed by the cumulant method and the mean characteristic time width, $\bar{\Gamma}$, was obtained.

The effective or mutual diffusion coefficient, D, can be evaluated by a relation of $D \equiv \bar{\Gamma}/\mu^2$. The mutual diffusion coefficient is a function of scattering angle and micelle concentration, $c - c_o$, that is

$$D = D'_d(\mu)D'_i(c-c_o,\mu)$$
$$= D'_d(\mu)[1 - (\bar{v} + k_f)(c - c_o)]MK(c - c_o)/(R_\theta - R_\theta^\circ) \quad (1)$$

where D'_d and D'_i are the terms associated with the diffusion coefficients and the intra- and interparticle interference effects, respectively. $\bar{v}$ is the partial specific volume of a micelle, and k_f is the frictional virial coefficient. M is the molecular weight of a micelle, K is the optical constant of the static light scattering, and R and R° are the reduced scattering intensities at the surfactant concentration, c, and the critical micelle concentration, c_o, respectively.

Results

Figures 1 and 2 show the scattering vector dependence of mutual diffusion coefficients for 4 M NaCl solutions of $C_{12}E_7$, 3 M NaCl solutions of $C_{14}E_7$, and 1 and 2 M NaCl solutions of $C_{16}E_7$ at 25 °C. For dilute solutions of micelles, mutual diffusion coefficients increase linearly with an increase in μ^2. When micelle concentrations are increased, the initial straight line in a plot of mutual diffusion coefficients against μ^2 deviates downward at high scattering vectors.

As micelle concentrations are increased further, the upward deviation at low scattering vectors also manifests. The deviation

(1) Flamberg, A.; Pecora, R. *J. Phys. Chem.* **1984**, *88*, 3026.
(2) Wilcoxon, J. P.; Kaler, E. W. *J. Chem. Phys.* **1987**, *86*, 4684.
(3) Pecora, R. *J. Chem. Phys.* **1968**, *48*, 4126; *Ibid.* **1968**, *49*, 1032.
(4) Berne, B. J.; Pecora, R. *Dynamic Light Scattering*; Wiley: New York, 1976.
(5) Zero, K. M.; Pecora, R. *Macromolecules* **1982**, *15*, 87.
(6) Aragõn, S. R.; Pecora, R. *Macromolecules* **1985**, *18*, 1868.
(7) Maeda, T.; Fujime, S. *Macromolecules* **1984**, *17*, 2381.
(8) Fujime, S.; Maeda, T. *Macromolecules* **1985**, *18*, 191.
(9) Fujime, S.; Takasaki-Ohsita, M.; Maeda, T. *Macromolecules* **1987**, *20*, 1292.
(10) Kubota, K.; Tominaga, Y.; Fujime, S. *Macromolecules* **1986**, *19*, 1604.
(11) Imae, T. *J. Phys. Chem.* **1988**, *92*, 5721.
(12) Imae, T.; Sasaki, M.; Ikeda, S. *J. Colloid Interface Sci.* **1989**, *127*, 511.
(13) Imae, T. *Langmuir* **1989**, *5*, 205.
(14) Sasaki, M.; Imae, T.; Ikeda, S. *Langmuir* **1989**, *5*, 211.
(15) Imae, T.; Sasaki, M.; Abe, A.; Ikeda, S. *Langmuir* **1988**, *4*, 414.
(16) Imae, T. *J. Colloid Interface Sci.* **1989**, *127*, 256.

0022-3654/89/2093-6720$01.50/0

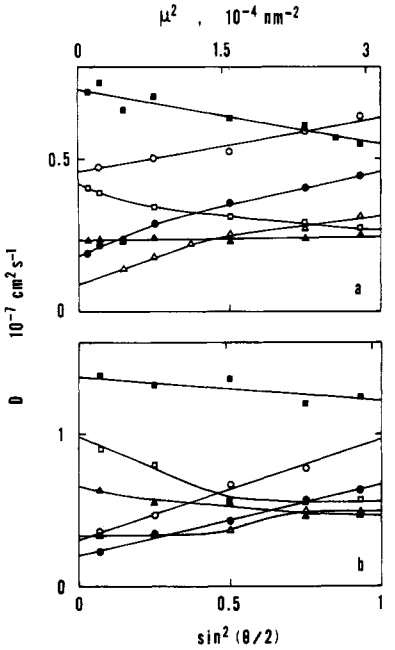

Figure 1. Scattering vector dependence of mutual diffusion coefficients for aqueous NaCl solutions of C_nE_7 at 25 °C. (a) $C_{12}E_7$ in 4 M NaCl. Micelle concentration (10^{-2} g cm^{-3}): ○, 0.21; ●, 0.43; △, 1.24; ▲, 3.03; □, 5.03; ■, 7.55. (b) $C_{14}E_7$ in 3 M NaCl. Micelle concentration (10^{-2} g cm^{-3}): ○, 0.20; ●, 0.42; △, 1.21; ▲, 3.00; □, 4.92; ■, 7.49.

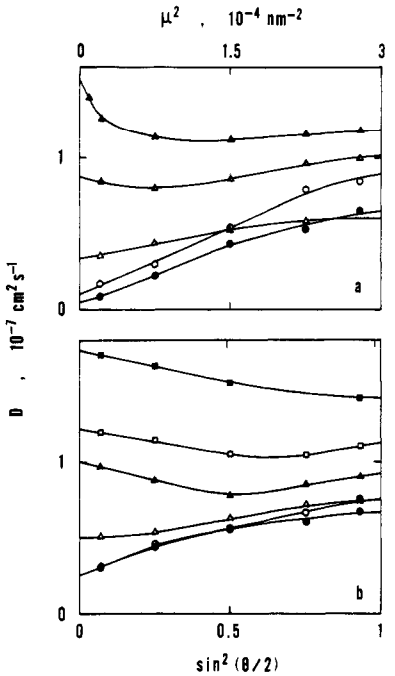

Figure 2. Scattering vector dependence of mutual diffusion coefficients for aqueous NaCl solutions of $C_{16}E_7$ at 25 °C. (a) In 1 M NaCl. Micelle concentration (10^{-2} g cm^{-3}): ○, 0.20; ●, 0.40; △, 1.19; ▲, 2.00; ▲, 2.94. (b) In 2 M NaCl. Micelle concentration (10^{-2} g cm^{-3}): ○, 0.21; ●, 0.40; △, 1.21; ▲, 2.94; □, 5.00; ■, 7.00.

at low scattering vectors becomes stronger with a further increase in micelle concentration and, at last, mutual diffusion coefficients decrease with an increase in μ^2 over all scattering vectors examined.

The scattering vector dependence of mutual diffusion coefficients was also observed for 4 M NaCl solutions of $C_{10}E_7$, 3 and 3.5 M NaCl solutions of $C_{12}E_7$, 1 and 2 M NaCl solutions of $C_{14}E_7$, and 0 and 0.1 M NaCl solutions of $C_{16}E_7$. The variation of the dependence is more intensive at high NaCl concentrations and for surfactants with a longer alkyl chain.

The scattering vector dependence of mutual diffusion coefficients is more remarkable for 2.6 M NaCl solutions of $C_{14}DAC$

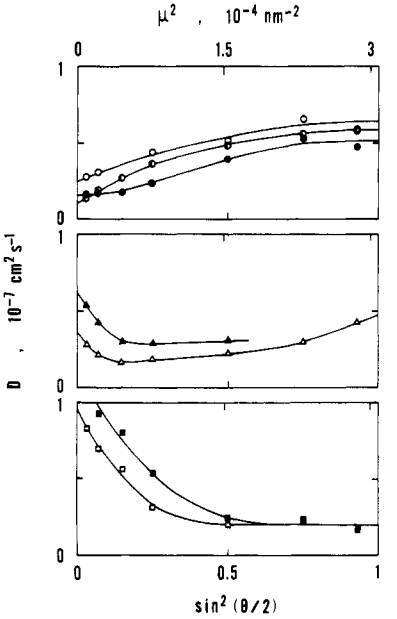

Figure 3. Scattering vector dependence of mutual diffusion coefficients for aqueous 2.6 M NaCl solutions of $C_{14}DAC$ at 30 °C. Micelle concentration (10^{-2} g cm^{-3}): ○, 0.095; ◐, 0.20; ●, 0.48; △, 0.95; ▲, 1.94; □, 2.93; ■, 4.03.

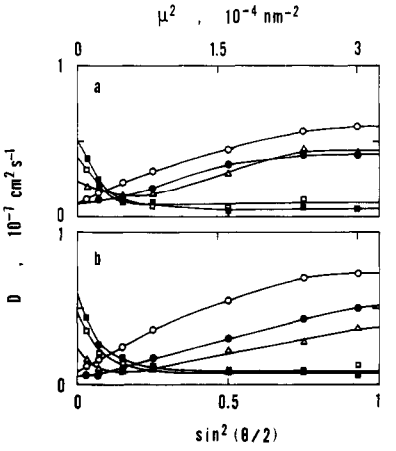

Figure 4. Scattering vector dependence of mutual diffusion coefficients for aqueous 4.3 M NaBr solutions of $C_{14}DAB$ at 25 and 35 °C. (a) 25 °C; (b) 35 °C. Micelle concentration (10^{-2} g cm^{-3}): ○, 0.19; ●, 0.53; △, 1.04; □, 2.00; ■, 3.01.

at 30 °C and 4.3 M NaBr solutions of $C_{14}DAB$ at 25 and 35 °C, as seen in Figures 3 and 4. The figure for 2.6 M NaCl solutions of $C_{14}DAC$ at 20 °C is given in ref 13. Even at micelle concentrations of (0.1–0.2) × 10^{-2} g cm^{-3}, mutual diffusion coefficients increase with curvature, except at low scattering vectors, and some of the curves reach constant values at high scattering vectors.

The initial decrease on plots of mutual diffusion coefficients against μ^2 is observed at higher micelle concentrations than 0.5 × 10^{-2} g cm^{-3}, and curves exhibit constant values at high scattering vectors for solutions with higher micelle concentrations.

Even if the temperature rises from 20 to 40 °C for $C_{14}DAC$ and from 25 to 45 °C for $C_{14}DAB$, the scattering vector dependence of mutual diffusion coefficients does not change severely.

Discussion

The patterns on plots of mutual diffusion coefficients against μ^2 for aqueous sodium halide solutions of C_nE_7, $C_{14}DAC$, and $C_{14}DAB$ can be classified into several types, depending on micelle concentration. (a) The mutual diffusion coefficients increase linearly with an increase in μ^2 over all ranges of scattering vectors examined. (b) At high scattering vectors, mutual diffusion coefficients deviate downward from an initial straight line and sometimes constrict to a constant value. (c) The mutual diffusion

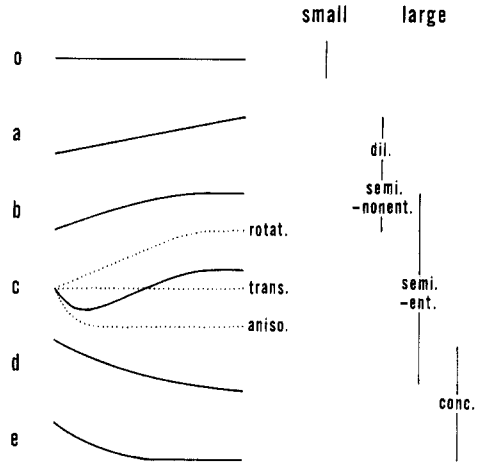

Figure 5. Observed typical and theoretical patterns on plots of mutual diffusion coefficients against μ^2 and participation with micelle size and regimes of micelle concentration.

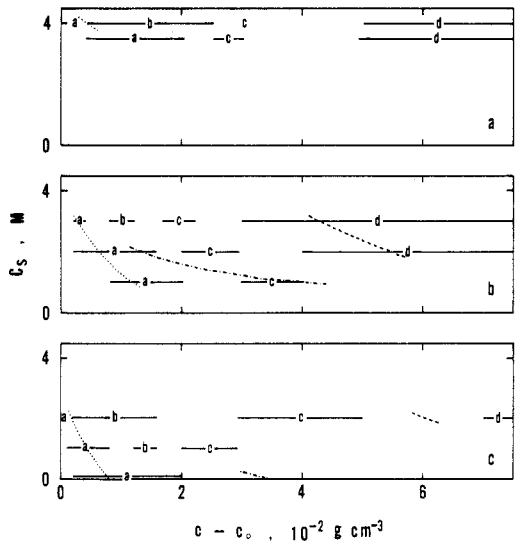

Figure 6. Diagrams of patterns a–d for aqueous sodium halide solutions of C_nE_7 at 25 °C as a function of NaCl concentration vs micelle concentration. (a) $C_{12}E_7$; (b) $C_{14}E_7$; (c) $C_{16}E_7$. Bars at both sides of each letter represent a range for micelle concentration of a corresponding pattern. ···, threshold micelle concentration of overlap; –·–, threshold micelle concentration of entanglement; - - -, crossover concentration between semidilute and concentrated regimes.

coefficients deviate upward at low scattering vectors. Therefore, a curve decreases initially and then increases through minimum. (d) The minimum and the succeeding increase at high scattering vectors disappear and mutual diffusion coefficients decrease monotonously over all scattering vectors. (e) The mutual diffusion coefficients decrease steeply at low scattering vectors and become constant at high scattering vectors. The typical patterns are illustrated in Figure 5.

NaCl and micelle concentrations where patterns a–e are revealed are represented in Figure 6 for aqueous NaCl solutions of C_nE_7 at 25 °C. The same kind of diagrams against temperatures and micelle concentrations are given in Figure 7 for 1 M NaCl solutions of $C_{14}E_7$, 2.6 M NaCl solutions of $C_{14}DAC$, and 4.3 M NaBr solutions of $C_{14}DAB$.

Figures 6 and 7 also illustrate threshold micelle concentrations for overlap and entanglement of rodlike micelles. The threshold values above which rodlike micelles overlap one another were calculated on the basis of a wormlike chain model,[17] and threshold values above which rodlike micelles entangle were obtained from a viscometric measurement.[12,14] The crossover concentrations between semidilute and concentrated regimes were observed on

(17) Imae, T. *Colloid Polym. Sci.*, in press.

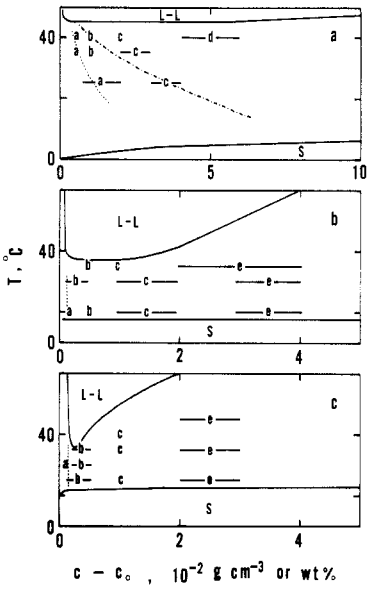

Figure 7. Diagrams of patterns a–e for aqueous sodium halide solutions of $C_{14}E_7$, $C_{14}DAC$, and $C_{14}DAB$ as a function of temperature vs micelle concentration. (a) $C_{14}E_7$ in 1 M NaCl; (b) $C_{14}DAC$ in 2.6 M NaCl; (c) $C_{14}DAB$ in 4.3 M NaBr. L–L, liquid–liquid phase separation; s, separation of solid. The phase diagram is given by a micelle concentration of weight percent. The other symbols have same meanings as those in Figure 6.

a light scattering analysis[11] and are included in Figure 6.

Aqueous sodium halide solutions of $C_{14}E_7$, $C_{14}DAC$, and $C_{14}DAB$ display phase separation, that is, the liquid–liquid phase separation at high temperatures and the separation of solid at low temperatures.[15] Figure 7 includes phase diagrams for aqueous sodium halide solutions of $C_{14}E_7$, $C_{14}DAC$, and $C_{14}DAB$.

When micelle concentrations which present each pattern on plots of mutual diffusion coefficients against μ^2 are compared with dilute, semidilute, and concentrated regimes of rodlike micelles, it is ascertained from Figures 6 and 7 that patterns a and b are observed at the dilute regime and the semidilute but nonentangled regime. The patterns b–d are mainly obtained at the semidilute and entangled regime, and patterns d and e belong to the concentrated regime. The participation between patterns and regimes of micelle concentration is given in Figure 5.

The mutual diffusion coefficients consist of terms associated with the diffusion coefficients and the interference effects, as described by (1). The contribution from these terms depends on the size and shape of micelles and regimes of micelle concentration.

1. The mutual diffusion coefficients for small micelles are independent of scattering vector, as shown in pattern 0 of Figure 5. The values are related to the total translational diffusion coefficient, D_o, as follows:

$$D = D_o[1 + k_D(c - c_o)] \quad (2)$$

where k_D is the hydrodynamic virial coefficient.[18]

Usually, spherical micelles are small; their aggregation numbers are around 50–100. For such small micelles, any scattering vector dependence of mutual diffusion coefficients was not observed and mutual diffusion coefficients obeyed (2).[16]

2. For large micelles but at small $R_G^2\mu^2$, mutual diffusion coefficients are described by

$$D = D_o(1 + AR_G^2\mu^2)[1 + k_D(c - c_o)] \quad (3)$$

where R_G is the radius of gyration of a micelle and A is a constant.[19,20] Therefore, mutual diffusion coefficients increase linearly with μ^2, as seen in pattern a of Figure 5, and numerical values of R_G and $D_o[1 + k_D(c - c_o)]$ are given by the slope of a straight

(18) Yamakawa, H. *Modern Theory of Polymer Solution*; Harper and Row: New York, 1971; p 181.
(19) Burchard, W.; Schmidt, M.; Stockmayer, W. H. *Macromolecules* **1980**, *13*, 580.
(20) Burchard, W. *Adv. Polym. Sci.* **1983**, *48*, 1.

line and the extrapolation to zero scattering vector.

The dynamic light scattering has been measured for rodlike micelles in aqueous sodium halide solutions and analyzed at small $R_G^2\mu^2$ on the basis of (3).[11,13]

3. For long semiflexible rodlike micelles and at large $R_G^2\mu^2$, it is ensured that theoretical equations for the mutual diffusion coefficient are different at dilute, semidilute, and concentrated regimes, according to a transcription of a theory for long semiflexible polymer chains.[7-9]

3.1. In dilute solutions of $(c - c_o) \leq (c - c_o)^*$, where $(c - c_o)^*$ is a threshold micelle concentration of overlap, the diffusion coefficient term of the mutual diffusion coefficient can be written by

$$D'_d(\mu) = D_o + (L_c^2/12)\theta_r f_1^*(k) + (D_\parallel - D_\perp)[f_2^*(k) - 1/3] \quad (4)$$

where L_c is the contour length of a rodlike micelle. θ_r is the rotational diffusion coefficient. $D_\perp$ and $D_\parallel$ are translational diffusion coefficients perpendicular and parallel to the rod axis, respectively, and have a relation of

$$D_o = (D_\parallel + 2D_\perp)/3 \quad (5)$$

$f_1^*(k)$ and $-3[f_2^*(k) - 1/3]$ are functions of $k = \mu L_c/2$ and the persistence length, a, of a semiflexible rodlike micelle. Their numerical values are zero at $\mu \to 0$, are unity at $\mu \to \infty$, and increase with k at $0 < \mu < \infty$. Therefore, the diffusion coefficient term of the mutual diffusion coefficient depends on the k value or on the scattering vector; that is, the second term in (4) increases and the third term decreases with the scattering vector, while the first term is independent of the scattering vector. The theoretically estimated pattern for each term is drawn in Figure 5.

At limits of $\mu \to 0$ and $\mu \to \infty$, respectively

$$\lim_{\mu \to 0} D'_d(\mu) \equiv D'_d(0) = D_o \quad (6)$$

and

$$\lim_{\mu \to \infty} D'_d(\mu) \equiv D'_d(\infty) \approx D_o + (L_c^2/12)\theta_r - (D_\parallel - D_\perp)/3$$

$$= D_\perp + (L_c^2/12)\theta_r \quad (7)$$

If it is supposed that the contribution from the anisotropy of the translational diffusion is much smaller than those from the total translational diffusion and the rotational diffusion, the difference

$$\Delta D'_d(\infty) \equiv D'_d(\infty) - D'_d(0) \approx (L_c^2/12)\theta_r \quad (8)$$

should be positive. Then the $D'_d(\mu)$ values increase gradually with μ^2 and constrict to a constant value at $\mu \to \infty$, as seen in pattern b in Figure 5.

3.2. In the semidilute regime which is defined by $(c - c_o)^* \leq (c - c_o) \leq (c - c_o)^{**}$, where $(c - c_o)^{**}$ is a crossover concentration between semidilute and concentrated regimes, the diffusion coefficient term of the mutual diffusion coefficient can be described in the same equation as that for dilute solutions,[9] that is

$$D'_d(\mu) = D_{sd,o} + (L_c^2/12)\theta_{r,sd} f_1^*(k) + (D_{sd,\parallel} - D_{sd,\perp})[f_2^*(k) - 1/3] \quad (9)$$

where the suffix sd means that parameters with this suffix belong to semidilute solutions.

It is expected in the semidilute regime that the rotational diffusion and the perpendicular translational diffusion are restricted.[9] Then

$$\theta_{r,sd} = \beta\theta_r, \quad D_{sd,\perp} = \beta' D_\perp, \quad \text{and} \quad D_{sd,\parallel} = D_\parallel \quad (10)$$

where $\beta, \beta' \leq 1$. Therefore

$$D'_d(0) = D_{sd,o} = (D_\parallel + 2\beta' D_\perp)/3 \quad (11)$$

$$D'_d(\infty) \approx D_{sd,o} + (L_c^2/12)\beta\theta_r - (D_\parallel - \beta' D_\perp)/3 \quad (12)$$

and

$$\Delta D'_d(\infty) \approx (L_c^2/12)\beta\theta_r - (D_\parallel - \beta' D_\perp)/3 \quad (13)$$

As the micelle concentration is increased, the scattering vector dependence of the $D'_d(\mu)$ values change complicatedly from pattern b to d through pattern c, owing to the compensation of contributions by the rotational diffusion and the anisotropy of the translational diffusion. Then numerical values of β and/or β' decrease from unity, and the difference, $\Delta D'_d(\infty)$, changes from positive to negative, whereas the $\Delta D'_d(\infty)$ value is zero at

$$(D_\parallel - \beta' D_\perp)/3 = (L_c^2/12)\beta\theta_r \quad (14)$$

3.3. For concentrated solutions of $(c - c_o)^{**} \leq (c - c_o)$, in the same way

$$D'_d(\mu) = D_{c,o} + (L_c^2/12)\theta_{r,c} f_1^*(k) + (D_{c,\parallel} - D_{c,\perp})[f_2^*(k) - 1/3] \quad (15)$$

and

$$\theta_{r,c} = \beta\theta_r, \quad D_{c,\perp} = \beta' D_\perp, \quad D_{c,\parallel} = D_\parallel, \quad \text{and} \quad \beta, \beta' \leq 1 \quad (16)$$

by using parameters with a suffix c, which represents "concentrated".

In this region, the rotational diffusion and the perpendicular translational diffusion are depressed strictly, enough to satisfy a condition of

$$(D_\parallel - \beta' D_\perp)/3 > (L_c^2/12)\beta\theta_r \quad (17)$$

Then at limits of $\beta, \beta' \to 0$

$$D'_d(0) = D_{c,o} \approx D_\parallel/3 \quad (18)$$

$$D'_d(\infty) \approx 0 \quad (19)$$

$$\Delta D'_d(\infty) \approx -D_\parallel/3 \quad (20)$$

Therefore, as seen in patterns d and e in Figure 5, the $D'_d(\mu)$ values decrease gradually with μ^2 and constrict to a constant value at $\mu \to \infty$, since contributions by the total translational diffusion and its anisotropy are dominant. Concurrently the difference, $\Delta D'_d(\infty)$, decreases with an increase in micelle concentration or with a more remarkable entanglement of rodlike micelles, until a value of $-D_\parallel/3$ is reached.

Figure 8 plots the difference $D(\theta{=}180) - D(\theta{=}0) = \Delta D(180)$ as a function of micelle concentration for aqueous sodium halide solutions of C_nE_7, C_{14}DAC, and C_{14}DAB. This parameter becomes a measure to compare contributions by the rotational diffusion and the anistropy of the translational diffusion at $\mu = 2\pi\tilde{n}_o/\lambda$, including the contributions from the interference effects.

For all systems, the $\Delta D(180)$ values display positive and maximum around the micelle concentration where the apparent micelle aggregation number is largest in dilute solutions.[11,13] At these micelle concentrations the rotational diffusion must mainly contribute, as discussed in 3.1.

The $\Delta D(180)$ values decrease gradually with increasing further the micelle concentration and become negative at high micelle concentrations. This change must indicate that the contribution by the rotational diffusion or the perpendicular translational diffusion decreases, as rodlike micelles entangle harder in semidilute and concentrated regimes, as described in 3.2 and 3.3.

The scattering vector dependence of mutual diffusion coefficients sometimes constricts to a constant value at large scattering vectors, as illustrated in pattern b or e of Figure 5. In such a case, the $\Delta D(180)$ value is equal to a difference

$$\lim_{\mu \to \infty} D - \lim_{\mu \to 0} D \equiv D(\infty) - D(0) \equiv \Delta D(\infty) \quad (21)$$

Such values are marked by the filled symbols in Figure 8.

Pattern b was observed for aqueous sodium halide solutions of C_{14}DAC and C_{14}DAB around micelle concentrations with the largest apparent micelle aggregation number in dilute solutions.[13] The obtained $D(0)$, $D(\infty)$, and $\Delta D(\infty)$ values are listed in Table I. The $\Delta D(\infty)$ values range to $(0.22\text{–}0.65) \times 10^{-7}$ cm^2 s^{-1}. They are maximum at a micelle concentration with the largest apparent micelle aggregation number and are larger at lower temperature.

TABLE I: Characteristics of Semiflexible Rodlike Micelles in Dilute Regime

	T, °C	$10^2(c - c_o)$, g cm^{-3}	$10^7D(0)$, cm^2 s^{-1}	$10^7D(\infty)$, cm^2 s^{-1}	$10^7\Delta D(\infty)$, cm^2 s^{-1}	L_c,[a] nm	a,[a] nm	θ_r, s^{-1}	10^7D_o,[a] cm^2 s^{-1}	$10^7(L_c^2/12)\theta_r$, cm^2 s^{-1}	$10^7[-(D_\parallel - D_\perp)/3]$, cm^2 s^{-1}
C_{14}DAC in 2.6 M NaCl	20	0.483	0.17	0.50	0.33						
	30	0.095	0.26	0.64	0.38						
		0.203	0.11	0.59	0.48	3610	48.4	79	0.16	8.6	0.009
		0.483	0.16	0.52	0.36						
C_{14}DAB in 4.3 M NaBr	25	0.111	0.16	0.60	0.44						
		0.191	0.10	0.59	0.49	2500	66.1	79	0.13	4.1	0.001
		0.532	0.09	0.42	0.33						
		1.036	0.23	0.45	0.22						
	30	0.191	0.10	0.64	0.55	3360	50.2	90	0.13	8.4	0.006
	35	0.191	0.08	0.73	0.65	5580	42.6	42	0.11	11.0	0.012

[a] From ref 17.

TABLE II: Characteristics of Semiflexible Rodlike Micelles in Semidilute or Concentrated Regime

	T, °C	$10^2(c - c_o)$, g cm^{-3}	$10^7D(0)$, cm^2 s^{-1}	$10^7D(\infty)$, cm^2 s^{-1}	$10^7\Delta D(\infty)$, cm^2 s^{-1}	$\Delta D(\infty)/D(0)$
C_{14}DAC in 2.6 M NaCl	20	2.927	0.80	0.30	−0.50	−0.63
		4.029	1.23	0.16	−1.07	−0.87
		5.946	1.67	0.41	−1.26	−0.75
	30	2.927	0.96	0.20	−0.76	−0.79
		4.029	1.21	0.21	−1.00	−0.83
	40	1.943	0.60	0.29	−0.32	−0.53
		2.927	0.94	0.30	−0.64	−0.68
		4.029	1.05	0.34	−0.72	−0.68
C_{14}DAB in 4.3 M NaBr	25	2.001	0.39	0.09	−0.31	−0.78
		3.011	0.50	0.05	−0.45	−0.90
	35	2.001	0.47	0.09	−0.39	−0.82
		3.011	0.58	0.08	−0.51	−0.87
	45	2.001	0.30	0.10	−0.20	−0.67
		3.011	0.42	0.09	−0.33	−0.79

The $\Delta D'_d(\infty)$ values for dilute solutions of semiflexible rodlike micelles correspond to

$$\Delta D'_d(\infty) = D(\infty)/D'_i(c-c_o,\infty) - D(0)/D'_i(c-c_o,0) \approx (L_c^2/12)\theta_r \quad (22)$$

according to (1) and (8). If numerical values observed and evaluated previously[13,17] are used for the evaluation of the $D'_i(c-c_o,\mu)$ values, the rotational diffusion coefficient can be calculated, as listed in Table I. In Table I, the numerical values of the contour length and the persistence length are also included. The evaluated rotational diffusion coefficients are 42–90 s^{-1} for rodlike micelles with contour lengths of 2500–5580 nm.

The equation of the rotational diffusion coefficient for semiflexible polymer chains was derived by Hagerman and Zimm.[21] However, the equation is valid to polymer chains with $0.05 < L_c/2a < 2.5$, while the $L_c/2a$ values for rodlike micelles of C_{14}DAC and C_{14}DAB examined here are too large. Actually, the numerical values of the rotational diffusion coefficient calculated by their equation are not reasonable for rodlike micelles of C_{14}DAC and C_{14}DAB.

Flamberg and Pecora[1] measured the dynamic light scattering for 4 M NaCl solution of dodecyldimethylammonium chloride at 25 °C and evaluated the translational diffusion coefficient of 0.32×10^{-7} cm^2 s^{-1} and the rotational diffusion coefficient of 1300 s^{-1} for rodlike micelles of $L_c = 460$ nm, $a = 82$ nm, and $r = 2.05$ nm, where r is the radius of a cross section of a rod.

Zhou et al.[22] determined the rotational diffusion coefficient of long polymer chains formed by cobalt monooleate soap molecules, by using the transient electric birefringent technique. Soap polymer chains of $L_c = 237$ nm and $a = 108$ nm exhibited the rotational diffusion coefficient of 32 s^{-1}.

The equation of the field correlation function by Fujime and Maeda[7,8] was applied to dilute solutions of poly(γ-benzyl L-glutamate)s. Kubota et al.[10] obtained the rotational diffusion coefficients of ~3000 and ~1800 s^{-1} for polymers of $a = 156.5$ nm and $r = 1.1$ nm with L_c of 205 and 255 nm, respectively.

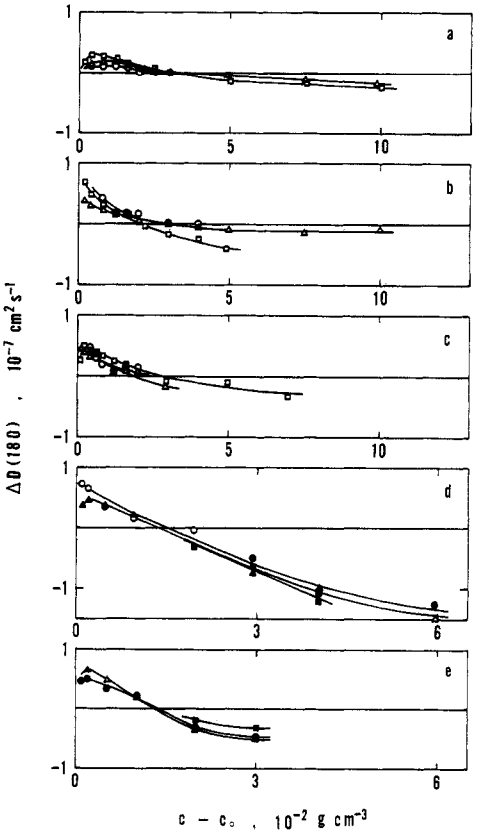

Figure 8. The difference, $\Delta D(180)$, as a function of micelle concentration for aqueous sodium halide solutions of C_nE_7, C_{14}DAC, and C_{14}DAB. (a) Aqueous NaCl solutions of $C_{12}E_7$ at 25 °C. NaCl concentration (M): ○, 3; △, 3.5; □, 4. (b) Aqueous NaCl solutions of $C_{14}E_7$ at 25 °C. NaCl concentration (M): ○, 1; △, 2; □, 3. (c) Aqueous NaCl solutions of $C_{16}E_7$ at 25 °C. NaCl concentration (M): ○, 0; △, 1; □, 2. (d) 2.6 M NaCl solutions of C_{14}DAC. Temperature (°C): ○, 20; △, 30; □, 40. (e) 4.3 M NaBr solutions of C_{14}DAB. Temperature (°C): ○, 25; △, 35; □, 45. The filled symbols represent the $\Delta D(\infty)$ values.

(21) Hagerman, P. J.; Zimm, B. H. *Biopolymers* **1981**, *20*, 1481.
(22) Zhou, Z.; Georgalis, Y.; Llang, W.; Li, J.; Xu, R.; Chu, B. *J. Colloid Interface Sci.* **1987**, *116*, 473.

The rotational diffusion coefficients for rodlike micelles of C_{14}DAC and C_{14}DAB are smaller than those of dodecyldimethylammonium chloride and poly(γ-benzyl L-glutamate)s, depending on the long contour length.

Schmidt and Stockmayer[23] presented approximately an equation

$$D_{\parallel} - D_{\perp} = (3/4)D_0[1 - 0.5(L_c/2a)^{1/4}] \quad (23)$$

for semiflexible polymer chains. If (23) is transcribed to semiflexible rodlike micelles, the contribution by the anisotropy of the translational diffusion, which is omitted in (8), can be described by

$$-(D_{\parallel} - D_{\perp})/3 = -(1/4)D_0[1 - 0.5(L_c/2a)^{1/4}] \quad (24)$$

Numerical values can be calculated by using the contour length and persistence length of rodlike micelles and the translational diffusion coefficient listed in Table I. The $-(D_{\parallel} - D_{\perp})/3$ values are definitely small in comparison with the D_0 and $(L_c^2/12)\theta_r$ values, as seen in Table I. This proves that the assumption of the negligible contribution by the anisotropy of the translational diffusion in (7) is reasonable.

At high micelle concentrations above 2×10^{-2} g cm^{-3} which belong to the semidilute or concentrated regime, mutual diffusion coefficients for 2.6 M NaCl solutions of C_{14}DAC and 4.3 M NaBr solutions of C_{14}DAB reached a constant value at high μ^2. Constant values are listed in Table II, where the $D(0)$ and $\Delta D(\infty)$ values are also included. The $\Delta D(\infty)$ values are negative, and their absolute values increase with an increase in micelle concentration, independent of the temperature.

The $\Delta D'_d(\infty)$ values in the semidilute and concentrated regimes change from (13) to (20), with increasing micelle concentration. At the high limit of micelle concentration, where the rotational diffusion and the perpendicular translational diffusion are restricted

$$\Delta D(\infty)/D(0) = D'_d(\infty)D'_i(c-c_0,\infty)/D'_d(0)D'_i(c-c_0,0) - 1 \approx -1 \quad (25)$$

from (1) and (19). The $\Delta D(\infty)/D(0)$ values were calculated and included in Table II. They approach -1 as micelle concentrations are increased.

It is stated that, in solutions of rodlike molecules at higher concentrations, the field correlation functions at nonzero scattering angles decay in a double-exponential fashion.[24] It is due to the coupling of the restricted rotational diffusion to the translational diffusion, in which the perpendicular translational diffusion is precluded. Such non-single-exponential curves of the field correlation function at finite scattering angles were observed for aqueous sodium halide solutions of surfactants at the semidilute and concentrated regimes examined here. This observation must confirm that rodlike micelles in such surfactant solutions behave similar to the rodlike molecules at high concentrations.

Acknowledgment. I am grateful to Drs. S. Fujime and T. Maeda for their valuable suggestions to apply their theory.

(23) Schmidt, M.; Stockmayer, W. H. *Macromolecules* **1984**, *17*, 509.

(24) Schurr, J. M.; Schmitz, K. S. *Annu. Rev. Phys. Chem.* **1986**, *37*, 271.

Effect of Structural and Chemical Factors on the Acidity and IR Spectroscopic Characteristics of Bridging OH Groups in Zeolites

A. G. Pelmenshchikov, E. A. Paukshtis, V. G. Stepanov, V. I. Pavlov, E. N. Yurchenko, K. G. Ione, G. M. Zhidomirov,*

Institute of Catalysis, USSR Academy of Sciences, 630090 Novosibirsk 99, USSR

and S. Beran*,†

J. Heyrovský Institute of Physical Chemistry and Electrochemistry, Czechoslovak Academy of Sciences, Dolejškova 3, 18223 Prague, Czechoslovakia *(Received: November 8, 1988; In Final Form: March 14, 1989)*

The nonempirical method with an STO-3G basis set is used to study the effect of both the geometric (structural factor) and chemical (chemical factor) characteristics of bridging OH groups in zeolites on their acidity and vibrational frequencies. It is shown that the acid strength of the OH groups is especially affected by changes in the chemical factor, while the vibrational frequencies are particularly influenced by the changes in the structural factor. These conclusions following from quantum chemical calculations are supported by the results of the IR spectroscopic studies of the isosteric adsorption of ND_3 for a series of zeolites, as well as by the data of MAS NMR measurements.

Introduction

This study will be devoted to investigation of the reasons for heterogeneity of the acidic and IR spectroscopic characteristics of the bridging OH groups in zeolites. Beaumont and Barthomeuf have found[1,2] that the effective Brønsted acidity, α, of Al sites in the framework of faujasites (X, Y, and dealuminated) (i) increases with increasing Si/Al ratio, (ii) reaches a maximum, $\alpha = 1$, for Si/Al = 6, and (iii) remains constant with further increase in the Si/Al ratio. The stretching vibrational frequencies of these centers were found to exhibit analogical behavior: (i) an increase in the Si/Al ratio in these zeolites results in a shift of the high-frequency band, $\nu_{OH} = 3660$ cm^{-1}, to lower frequencies, (ii) a minimum value of frequency, $\nu_{OH} = 3630$ cm^{-1}, is attained for Si/Al = 6, and (iii) for an Si/Al ratio higher than 6, the vibrational frequency remains constant. It is well-known[3,4] that in dealuminated faujasites with Si/Al = 6 no Al atoms are located in the nearest possible positions to another Al atom. Therefore, these results indicate that substitution of Si for Al in the T site of the ≥Al–OH–(Si<)–O–(Si<)–O–T≤ and ≥Si–OH–(Al<)–O–(Si<)–O–(Si<)–O–T≤ fragments of the lattice does not in-

† Deceased.

(1) Beaumont, R.; Barthomeuf, D. *J. Catal.* **1972**, *26*, 218.
(2) Barthomeuf, D. In *Studies in Surface Science and Catalysis. 5. Catalysis by Zeolites*; Imelik, B., Ed.; Elsevier: Amsterdam, 1980; p 55.
(3) Beagley, B.; Dweyer, J.; Fitch, F. R.; Mann, R.; Walters, J. *J. Phys. Chem.* **1984**, *88*, 1744.
(4) Barthomeuf, D. *Mater. Chem. Phys.* **1987**, *17*, 49.

0022-3654/89/2093-6725$01.50/0